A LETTERS JOURNAL EXPLORING THE FRONTIERS OF PHYSICS

March 2017

EPL, **117** (2017) 57008
doi: 10.1209/0295-5075/117/57008

www.epljournal.org

Damping in a superconducting mechanical resonator

OREN SUCHOI and EYAL BUKS

Andrew and Erna Viterbi Department of Electrical Engineering, Technion - Haifa 32000, Israel

received 22 February 2017; accepted in final form 19 April 2017
published online 8 May 2017

PACS 74.25.Ld – Superconductivity: Mechanical and acoustical properties, elasticity, and ultrasonic attenuation
PACS 46.40.-f – Vibrations and mechanical waves

Abstract – We study a mechanical resonator made of aluminum near the normal-to-superconducting phase transition. A sharp drop in the rate of mechanical damping is observed below the critical temperature. The experimental results are compared with predictions based on the Bardeen Cooper Schrieffer theory of superconductivity and a fair agreement is obtained.

Mechanical resonators having low damping rate are widely employed for sensing and timing applications [1]. At sufficiently low temperatures such devices may allow the experimental exploration of the crossover from classical to quantum mechanics [2–8]. Commonly, the observation of non-classical effects in such experiments is possible only when the damping rate [9] of the mechanical resonator is sufficiently low. Mechanical resonators made of superconductors are widely employed in such low-temperature experiments. In this study we experimentally investigate the effect of superconductivity on the damping rate of a mechanical resonator made of aluminum near its normal-to-superconducting phase transition.

The damping rate can be measured by coupling the mechanical resonator under study to a displacement detector. In general, a variety of different mechanisms may contribute to the total mechanical damping rate. In order to isolate the effect of superconductivity it is important to employ a method of displacement detection that is unaffected by the normal-to-superconducting phase transition. In addition, systematic errors in the measured damping rate due to back-reaction effects originating from the coupling between the mechanical resonator and the displacement detector have to be kept at a sufficiently low level.

In our setup (see fig. 1) we employ the so-called optomechanical cavity configuration [10–12], in which displacement detection is performed by coupling the mechanical resonator to an electromagnetic cavity. While many of the previous studies of superconducting mechanical resonators have employed such a configuration with a superconducting microwave cavity [4,6,7,13–21], our setup, which is based on a cavity in the optical band, allows displacement detection that is unaffected by the phase transition

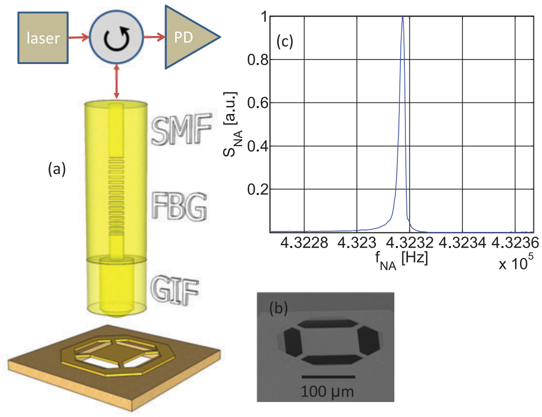

Fig. 1: (Colour online) The experimental setup. (a) A sketch of the mechanical resonator and the fiber-based optical cavity. (b) Electron micrograph of the trampoline. (c) The resonance lineshape of the fundamental mechanical mode.

occurring in the mechanical resonator under study, which, in-turn, allows isolating the effect of superconductivity on the mechanical damping. Moreover, back-reaction effects are suppressed by employing a relatively low driving power to the optical cavity (see discussion below). The magnetomotive scheme has been employed for displacement detection in ref. [22] in order to study the temperature dependence of linear and nonlinear damping rates of a mechanical resonator made of aluminum near the normal to superconducting phase transition. The results indicate a significant reduction in the damping rate in the superconducting phase [22].

In our setup the optomechanical cavity is formed between two mirrors, a stationary fiber Bragg grating (FBG) mirror and a movable mirror made of a mechanical resonator in the shape of a trampoline supported by four beams (see fig. 1(a)). A graded index fiber (GIF) spliced to the end of the single mode fiber (SMF) is employed for focusing. A cryogenic piezoelectric three-axis positioning system having sub-nanometer resolution is employed for manipulating the position of the optical fiber. A photolithography process is used to pattern a $t_{\mathrm{Al}} = 200\,\mathrm{nm}$ thick aluminum layer on top of a a $t_{\mathrm{SiN}} = 100\,\mathrm{nm}$ thick silicon nitride layer into the shape of a $100 \times 100\,\mu\mathrm{m}^2$ trampoline with four supporting beams (see fig. 1(b)). Details of the fabrication process can be found elsewhere [23]. Measurements are performed in a dilution refrigerator at a pressure well below 2×10^{-5} mbar. Another device on the same wafer, which is made in the shape of a microwave microstrip resonator, allows characterizing the surface resistance of the aluminum layer [23].

A tunable laser operating near the Bragg wavelength of the FBG together with an external attenuator are employed to excite the optical cavity. The optical power reflected off the cavity is measured by a photodetector (PD), which is connected to a network analyzer (NA). Actuation is performed by applying an alternating voltage (with a direct voltage offset) between the trampoline and a stationary electrode positioned $200\,\mu\mathrm{m}$ below it.

The fundamental mechanical mode is characterized by its frequency $\omega_{\mathrm{m}}/2\pi$ and damping rate γ_{m}. Both parameters can be extracted from the resonance lineshape of the measured NA signal S_{NA} *vs.* angular driving frequency ω_{NA} with a fixed driving amplitude (see fig. 1(c)). In the regime of linear response $S_{\mathrm{NA}}(\omega_{\mathrm{NA}})$ is expected to be given by

$$S_{\mathrm{NA}}\left(\omega_{\mathrm{NA}}\right) = \frac{S_{\mathrm{NA,R}}}{1 + \left(\frac{\omega_{\mathrm{NA}} - \omega_{\mathrm{m}}}{\gamma_{\mathrm{m}}}\right)^2}, \tag{1}$$

where $S_{\mathrm{NA,R}}$ is the value of $S_{\mathrm{NA}}(\omega_{\mathrm{NA}})$ at resonance, *i.e.* when $\omega_{\mathrm{NA}} = \omega_{\mathrm{m}}$.

The measured damping rate γ_{m} *vs.* temperature T, which is extracted from the NA data using eq. (1), is indicated by the crosses in fig. 2. The same procedure yields the mode's frequency $\omega_{\mathrm{m}}/2\pi = 432.318\,\mathrm{kHz}$, which is found to be almost a constant for the range of temperatures explored in this measurement (between 0.5 K and 1.3 K). As can be seen from fig. 2, the measured damping rate γ_{m} sharply drops as the temperature T is lowered below the value of 1.1 K. Note that at the same temperature of 1.1 K the resonance of the microwave microstrip resonator becomes visible, indicating thus that the critical temperature is $T_{\mathrm{c}} = 1.1\,\mathrm{K}$, as is expected from high quality aluminum layer. The data seen in fig. 2 is obtained by setting the laser power that is injected into the optical cavity to the value $P_{\mathrm{L}} = 3 \times 10^{-8}\,\mathrm{W}$.

In general, heating due to optical absorption by the aluminum layer may give rise to a systematic error in the measurement of γ_{m}. Two possible mechanisms are discussed below. The first one is due to back-reaction originating from the bolometric optomechanical coupling [24,25],

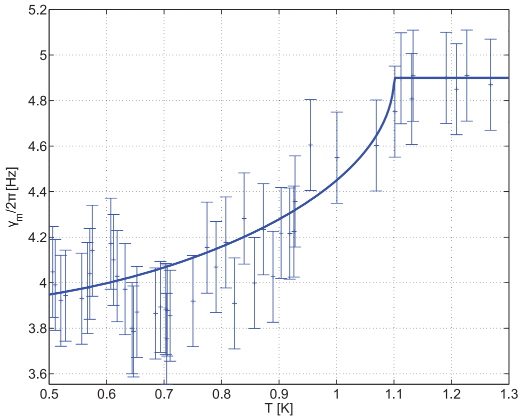

Fig. 2: (Colour online) The measured (crosses) and theoretically calculated (solid line) damping rate γ_{m} *vs.* temperature T. The calculated γ_{m} is obtained using eq. (2).

which gives rise to a shift in the effective value of γ_{m} denoted by $\gamma_{\mathrm{m,ba}}$. The magnitude of $\gamma_{\mathrm{m,ba}}$ can be roughly estimated using the relation $|\gamma_{\mathrm{m,ba}}|/\gamma_{\mathrm{m}} \simeq P_{\mathrm{L}}/P_{\mathrm{LT}}$, where P_{L} is the laser power that is employed for the measurement of γ_{m} and P_{LT} is the laser power at the threshold of self-excited oscillation [26]. For the same cavity tuning, for which the data seen in fig. 2 is obtained, self-excited oscillation occurs at a threshold power given by $P_{\mathrm{LT}} = 4 \times 10^5 P_{\mathrm{L}}$, and thus the effect of back-reaction can be safely disregarded.

The other possible source of a systematic error originates from temperature rise due to optical absorption. Due to the low heat conductance of both superconducting aluminum and silicon nitride, this mechanism imposes a severe upper limit upon the allowed values of laser power. The heating power is given by $P_{\mathrm{H}} = \zeta\beta_{\mathrm{F}}(1-R_{\mathrm{C}})P_{\mathrm{L}}$, where ζ is the absorption coefficient (for aluminum $\zeta = 0.03$), β_{F} is the cavity finesse, R_{C} is the cavity reflectivity, and P_{L} is the laser power [27]. For the measurement of γ_{m} that is presented in fig. 2 the optical cavity is tuned to have finesse of $\beta_{\mathrm{F}} = 1.8$ and reflectivity of $R_{\mathrm{C}} = 0.32$, and thus for this measurement $P_{\mathrm{H}} = 1.1 \times 10^{-9}\,\mathrm{W}$.

The temperature rise ΔT due to optical absorption is estimated by $\Delta T = P_{\mathrm{H}}/4K_{\mathrm{b}}$, where K_{b} is the thermal conductance of each of the four nominally identical beams that support the trampoline. The thermal conductance K_{b} is given by $K_{\mathrm{b}} = (t_{\mathrm{Al}}\kappa_{\mathrm{Al}} + t_{\mathrm{SiN}}\kappa_{\mathrm{SiN}})(w_{\mathrm{b}}/l_{\mathrm{b}})$, where κ_{Al} (κ_{SiN}) is the thermal conductivity of aluminum (silicon nitride), and where $w_{\mathrm{b}}/l_{\mathrm{b}} = 0.5$ is the ratio between width and length of the beams. For the lowest value of 0.5 K in the temperature range seen in fig. 2 the thermal conductivities are estimated to be $\kappa_{\mathrm{Al}} \simeq 4 \times 10^{-2}\,\mathrm{W\,K^{-1}\,m^{-1}}$ for aluminum [28] and $\kappa_{\mathrm{SiN}} \simeq 10^{-2}\,\mathrm{W\,K^{-1}\,m^{-1}}$ for silicon nitride [29,30]. For these values the estimated temperature rise is $\Delta T = 0.06\,\mathrm{K}$. For temperatures below 0.5 K the temperature rise ΔT becomes even larger since both κ_{Al} and κ_{SiN} rapidly drop at low temperatures, and therefore no reliable measurements can be obtained unless P_{H}

is further reduced. However, no significant reduction of P_H is possible in our setup due to noise, and consequently reliable data far below 0.5 K cannot be obtained. Note, however, that above 0.5 K no significant change in the damping rate is obtained when the measurements are repeated with a laser power two times higher, verifying thus that heating does not give rise to a significant systematic error in that range.

To account for the experimental results the measured damping rate γ_m is compared with theory. Let $\gamma_m = \gamma_e + \gamma_S$, where γ_e denotes the electronic contribution to the total rate of mechanical damping γ_m, and γ_S denotes the contribution of all other mechanisms. Well below the critical temperature the phonon energy $\hbar\omega_m$ becomes far smaller than the superconducting energy gap Δ, and consequently the electronic contribution γ_e is expected to drop well below its value in the normal phase, which is denoted by γ_N. The solid line seen in fig. 2 represents the calculated value of γ_m obtained from the following expression:

$$\gamma_m = \frac{2\gamma_N}{1 + \exp\frac{\Delta(T)}{k_B T}} + \gamma_S, \tag{2}$$

where the fitting parameters γ_S, γ_N and T_c are taken to be given by $\gamma_S/2\pi = 3.9$ Hz, $\gamma_N/2\pi = 1.0$ Hz and $T_c = 1.1$ K. The temperature dependence of γ_S is assumed to be negligibly small in the experimentally explored range between 0.5 K and 1.3 K. The first term in eq. (2) represents the temperature dependence of ultrasonic attenuation according to the Bardeen Cooper Schrieffer (BCS) theory [31,32], which is obtained using the golden rule formula in the limit where $\hbar\omega_m \ll \Delta$. The temperature-dependent energy gap $\Delta(T)$ is found by numerically solving the BCS gap equation [33]

$$\nu = \int_0^{\frac{e^\nu}{2\delta}} \mathrm{d}x\, \frac{\tanh\left(\frac{\xi\delta\sqrt{1+x^2}}{\tau}\right)}{\sqrt{1+x^2}}\,, \tag{3}$$

where $\nu = 1/gD_0$ is the inverse interaction strength with g being the electron-phonon coupling coefficient and D_0 being the density of states per unit volume, $\delta = \Delta/\Delta_0$ is the normalized gap with Δ_0 being the zero temperature gap, $\tau = T/T_c$ is the normalized temperature, and the number ξ is given by $\xi = \pi/2e^{C_E}$ with $C_E \simeq 0.577$ being Euler's constant. As can be seen from fig. 2, fair agreement between data and theory is obtained. A similar theoretical approach has been employed before to successfully account for the results of a measurement of a contact-less friction between a superconducting niobium film and a cantilever [34] (see also [35]).

The rate γ_N has been calculated in ref. [36] for the case where the electron mean-free path is greater than the wavelength of the oscillating acoustic mode. However, this assumption is not valid for our device. When the electron mean-free path is shorter than the acoustic wavelength the rate γ_N can be roughly estimated using Stokes' law of sound attenuation [37,38], which relates this rate to the electronic viscosity [39]. For the case of an acoustic wave having angular frequency ω_m propagating in a bulk aluminum the rate according to this approach is given by

$$\gamma_{N,\mathrm{bulk}} = \frac{2\eta_{Al}\omega_m^2}{3\rho_{Al}c_{Al}^2}, \tag{4}$$

where $\rho_{Al} = 2.7\,\mathrm{g\,cm^{-3}}$ and $c_{Al} = 5.1\times10^3\,\mathrm{m\,s^{-1}}$ are the mass density and the speed of sound, respectively, of aluminum, and where η_{Al} is the electronic viscosity of aluminum. The electronic viscosity can be expressed as $\eta_{Al} = (2/3)n_{Al}\tau_{Al}\langle\epsilon_{Al}\rangle$ where n_{Al} is the density of free electrons, τ_{Al} is the scattering relaxation time, and $\langle\epsilon_{Al}\rangle$ is the averaged kinetic energy (see eq. (43.8) in [40]). At low temperatures $\langle\epsilon_{Al}\rangle = 3\epsilon_{F,Al}/5$, where $\epsilon_{F,Al}$ is the Fermi energy. Using the values $n_{Al} = 18.1\times10^{22}\,\mathrm{cm^{-3}}$, $\tau_{Al} = 6.5\times10^{-14}$ s and $\epsilon_{F,Al} = 11.7$ eV [41] one obtains $\gamma_{N,\mathrm{bulk}} = 0.6$ Hz. This rough estimate, which disregards confinement, yields a value that is of the same order of magnitude as the value of $\gamma_N/2\pi = 1.0$ Hz that has been obtained above from the fitting of the data with eq. (2).

In summary, the contribution of free electrons to the damping rate of an aluminum mechanical resonator is measured. The behavior near the normal to superconducting phase transition is compared with a prediction based on the BCS theory. The relative contribution of free electrons in the normal state to the total damping rate of the resonator under study is found to be $\gamma_N/(\gamma_N+\gamma_S) = 0.20$.

* * *

This work was supported by the Israel Science Foundation, the Binational Science Foundation, the Security Research Foundation at Technion and the Russell Berrie Nanotechnology Institute.

REFERENCES

[1] Ekinci K. L. and Roukes M. L., *Rev. Sci. Instrum.*, **76** (2005) 061101.

[2] Meystre Pierre, *Ann. Phys. (Berlin)*, **525** (2013) 215.

[3] Poot M. and van der Zant H. S. J., *Phys. Rep.*, **511** (2012) 273.

[4] O'Connell A. D., Hofheinz M., Ansmann M., Bialczak Radoslaw C., Lenander M., Neeley Erik Luceroand M., Sank D., Wang H., Weides M., Wenner J., Martinis John M. and Cleland A. N., *Nature*, **464** (2010) 697.

[5] Pikovski Igor, Vanner Michael R., Aspelmeyer Markus, Kim M. S. and Brukner Časlav, *Nat. Phys.*, **8** (2012) 393.

[6] Weinstein A. J., Lei C. U., Wollman E. E., Suh J., Metelmann A., Clerk A. A. and Schwab K. C., *Phys. Rev. X*, **4** (2014) 041003.

[7] Teufel J. D., Donner Toblas, Li Dale, Harlow J. W., Allman M. S., Cicak K., Sirois A. J., Whittaker Jed D., Lehnert K. W. and Simmonds Raymond W., *Nature*, **475** (2011) 359.

[8] Chan Jasper, Mayer Alegre T. P., Safavi-Naeini Amir H., Hill Jeff T., Krause Alex, Gröblacher Simon, Aspelmeyer Markus and Painter Oskar, *Nature*, **478** (2011) 89.

[9] Unterreithmeier Quirin P., Faust Thomas and Kotthaus Jörg P., *Phys. Rev. Lett.*, **105** (2010) 027205.

[10] Braginsky V. B. and Manukin A. B., *Zh. Eksp. Teor. Fiz.*, **52** (1967) 986; *Sov. Phys. JETP*, **25** (1967) 653.

[11] Aspelmeyer Markus, Kippenberg Tobias J. and Marquardt Florian, *Rev. Mod. Phys.*, **86** (2014) 1391.

[12] Metcalfe Michael, *Appl. Phys. Rev.*, **1** (2014) 031105.

[13] Teufel J. D., Li Dale, Allman M. S., Cicak K., Sirois A. J., Whittaker J. D. and Simmonds R. W., *Nature*, **471** (2011) 204.

[14] Palomaki T. A., Teufel J. D., Simmonds R. W. and Lehnert K. W., *Science*, **342** (2013) 710.

[15] Yanai S., Singh V., Yuan M., Gely M., Bosman S. J. and Steele G. A., *Mechanical dissipation in more superconducting metal drums*, arXiv:1608.01871 (2016).

[16] Andrews R. W., Reed A. P., Cicak K., Teufel J. D. and Lehnert K. W., *Nat. Commun.*, **6** (2015) 10021.

[17] Lecocq F., Clark J. B., Simmonds R. W., Aumentado J. and Teufel J. D., *Phys. Rev. Lett.*, **116** (2016) 043601.

[18] Suh J., Shaw M. D., LeDuc H. G., Weinstein A. J. and Schwab K. C., *Nano Lett.*, **12** (2012) 6260.

[19] Wollman E. E., Lei C. U., Weinstein A. J., Suh J., Kronwald A., Marquardt F., Clerk A. A. and Schwab K. C., *Science*, **349** (2015) 952.

[20] Pirkkalainen J.-M., Damskägg E., Brandt M., Massel F. and Sillanpää M. A., *Phys. Rev. Lett.*, **115** (2015) 243601.

[21] Suchoi Oren, Shlomi Keren, Ella Lior and Buks Eyal, *Phys. Rev. A*, **91** (2015) 043829.

[22] Lulla K. J., Defoort Martial, Blanc Christophe, Bourgeois Olivier and Collin Eddy, *Phys. Rev. Lett.*, **110** (2013) 177206.

[23] Suchoi Oren, Ella Lior, Shtempluk Oleg and Buks Eyal, *Phys. Rev. A*, **90** (2014) 033818.

[24] Metzger C., Ludwig M., Neuenhahn C., Ortlieb A., Favero I., Karrai K. and Marquardt F., *Phys. Rev. Lett.*, **101** (2008) 133903.

[25] Zaitsev Stav, Pandey Ashok K., Shtempluck Oleg and Buks Eyal, *Phys. Rev. E*, **84** (2011) 046605.

[26] Dhayalan Yuvaraj, Baskin Ilya, Shlomi Keren and Buks Eyal, *Phys. Rev. Lett.*, **112** (2014) 210403.

[27] Shlomi Keren, Yuvaraj D., Baskin Ilya, Suchoi Oren, Winik Roni and Buks Eyal, *Phys. Rev. E*, **91** (2015) 032910.

[28] Feshchenko A. V., Saira O.-P., Peltonen J. T. and Pekola J. P., *Thermal conductance of nb thin films at sub-kelvin temperatures*, arXiv:1609.06519 (2016).

[29] Zink B. L. and Hellman F., *Solid State Commun.*, **129** (2004) 199.

[30] Woodcraft Adam L., Sudiwala Rashmi V., Wakui Elley, Bhatia Ravinder S., Bock James J. and Turner Anthony D., *Physica B: Condens. Matter*, **284** (2000) 1968.

[31] Persson B. N. J., *Solid State Commun.*, **115** (2000) 145.

[32] Claiborne Lewis T. jr. and Morse Robert W., *Phys. Rev.*, **136** (1964) A893.

[33] Bardeen John, Cooper Leon N. and Schrieffer John Robert, *Phys. Rev.*, **108** (1957) 1175.

[34] Kisiel Marcin, Gnecco Enrico, Gysin Urs, Marot Laurent, Rast Simon and Meyer Ernst, *Nat. Mater.*, **10** (2011) 119.

[35] Dayo A., Alnasrallah W. and Krim J., *Phys. Rev. Lett.*, **80** (1998) 1690.

[36] Lindenfeld Ze'ev and Lifshitz Ron, *Phys. Rev. B*, **87** (2013) 085448.

[37] Stokes G. G., *Trans. Cambridge Philos. Soc.*, **8** (1845) 287.

[38] Kittel C., *Rep. Prog. Phys.*, **11** (1947) 205.

[39] Heinisch Martin, Voglhuber-Brunnmaier Thomas, Reichel Erwin K., Dufour Isabelle and Jakoby Bernhard, *Sens. Actuators A: Phys.*, **220** (2014) 76.

[40] Kittel Charles, *Elementary Statistical Physics* (Courier Corporation) 2004.

[41] Ashcroft Neil W. and David N. Mermin, *Solid State Physics* (Saunders College, Philadelphia) 1976.